Revista Brasileira de Geofísica (2004) 22(3): 223-231

ISSN 0102-261X
www.scielo.br/rbg

COMPARISON OF THE OH (8-3) AND (6-2) BAND ROTATIONAL TEMPERATURE OF THE MESOSPHERIC AIRGLOW EMISSIONS

Cristiano Max Wrasse[1], Hisao Takahashi[2] and Delano Gobbi[3]

Recebido em 8 outubro, 2004 / Aceito em 10 novembro, 2004
Received October 8, 2004 / Accepted November 10, 2004

ABSTRACT. The airglow OH (8-3) and (6-2) band rotational temperatures were measured and compared using two scanning photometer at Cachoeira Paulista (23˚S, 45˚W) in 1999. The rotational temperature were obtained from the ratio between the $P_1(5)$ and $P_1(3)$ in the case of the (8-3) band and $P_1(4)$ and $P_1(2)$ lines for the (6-2) band. Three different Einstein coefficients, of Mies (1974), Langhoff et al., (1986) and Turnbull & Lowe (1989) were used and compared between them. It was shown that both the temperature did agree well with in an error range when the Langhoff et al.'s coefficients were used.

Keywords: Mesosphere, hydroxyl, rotational temperature, Einstein coefficients.

RESUMO. A temperatura rotacional das bandas da OH(8-3) e OH(6-2) foram medidas e comparadas utilizando dois fotômetros de filtro inclinável, em Cachoeira Paulista (23˚S, 45˚O) no ano de 1999. A temperatura rotacional foi determinada através da razão entre as linhas rotacionais $P_1(5)$ and $P_1(3)$ para o caso da banda (8-3) e entre as linhas rotacionais $P_1(4)$ e $P_1(2)$ para a banda (6-2). Os coeficientes de Einstein publicados por Mies (1974), Langhoff et al., (1986) e Turnbull & Lowe (1989) foram utilizados para o cálculo da temperatura e seus resultados foram comparados. Os resultados encontrados mostram que as temperaturas das bandas OH(8-3) e OH(6-2) são similares, dentro da margem de erro, quando os coeficientes de Einstein de Langhoff et al. foram utilizados.

Palavras-chave: Mesosfera, hidroxila, temperatura rotacional, coeficientes de Einstein.

Instituto Nacional de Pesquisas Espaciais (INPE), Caixa Postal: 515; CEP: 12245-970 – São José dos Campos, SP, Brasil. Phone: (12) 3945-7167; Fax: (12) 3945-6740.
[1]E-mail: cmw@laser.inpe.br
[2]E-mail: hisaotak@laser.inpe.br
[3]E-mail: delanogobbi@laser.inpe.br

INTRODUCTION

The airglow Hydroxyl emissions have been extensively used for studying atmospheric temperature variation in the mesopause region since Meinel (1950) published its usefulness (Greet et al., 1998, Bittner et al., 2000). The OH emission originates from a layer near 87 km of altitude with a thickness of around 8 km (Baker & Stair, 1988). The temperature in the mesopause region is highly variable, between 150 and 250 K, depending on the geographic location, local time, season and dynamical processes, such as tides and gravity waves (Waltersheid et al., 1987). The OH rotational temperature is one of useful parameters to monitor such variable atmospheric temperature in the mesopause region.

There are several reasons for using the OH rotational line spectrum to measure the mesopause temperature. The collision frequency of OH with the neutral atmosphere in the vicinity of 90 km of altitude should be in an order to $10^4 s^{-1}$ and the life time of the excited OH is around 3 to 10 msec. (Mies, 1974). It indicates that the excited OH molecules in the rotational energy levels are in a thermal equilibrium with the atmospheric ambient gas (Sivjee & Hamwey, 1987, Takahashi et al., 1998). The other reason to use the OH spectra is that the rotational line spectra is open structure, separating 1 to 2 nm between the lines, which makes easy to measure individual lines by even low resolution ($\sim$1 nm) spectrometer. Further, the line intensities of a band are only a function of the rotational temperature. Therefore using two lines from a single band one can estimate the rotational temperature by the following equation (Mies, 1974):

$$T_{n,m} = \frac{E_{v'}(J'_m) - E_{v'}(J'_n)}{k \ln\left[\frac{I_n}{I_m} \frac{A(J'_m, v' \rightarrow J''_{m+1}, v'')}{A(J'_n, v' \rightarrow J''_{n+1}, v'')} \frac{2J'_m+1}{2J'_n+1}\right]} \qquad (1)$$

Where $T_{n,m}$ is the rotational temperature estimated from two line intensities, I_n and I_m, from rotational levels J'_n, J'_m in the upper vibrational level v', to J''_{n+1}, J''_{m+1} in the lower vibrational level v''. $E_v(J)$ is the energy of the level (J, v). $A(J'_n, v' \rightarrow J''_{n+1}, v'')$ is the Einstein coefficient, for the transition from J'_n, v' to J''_m, v''.

The OH rotational temperatures have been measured using several different bands, for example, (9-4), (8-3), (6-2), (4-2) and (3-1) bands with a combination of different Einstein coefficients, Mies (1974) (hereafter Mies); Langhoff et al. (1986) (hereafter LWR); Turnbull & Lowe (1989) (hereafter TL); and Nelson et al. (1990). This different combination of measurement has been giving significant ambiguity in determination of the rotational temperature as pointed out by French et al. (2000). Table 1 shows recent OH temperature measurement carried out by different groups in the world.

It seems that the Einstein coefficients for the OH ground state and lower vibrational levels are consistent between the different calculations (Nelson et al., 1990). For the upper vibrational levels, however, the coefficients show a certain discrepancy between them. The relative intensities calculated by the TL coefficients are the highest and those calculated by LWR are the lowest (Golden, 1997). Calculation of the Einstein coefficients depends on precision of the electric dipole moment function and the wave function used. Error range of the two functions will increase in the higher vibrational and rotational levels. These are the factors that introduce discrepancy between the rotational temperatures.

Table 1 – OH temperature measurement by different groups, different bands and different Einstein coefficients.

Tabela 1 – *Temperatura da OH medida por diferentes grupos de pesquisas, utilizando diferentes bandas da OH e diferentes Coeficientes de Einstein.*

Author	Band	Coefficient
French et al. (2000)	OH (6-2)	LWR
Scheer & Reisin (2000)	OH (6-2)	Mies
Takahashi et al. (1999)	OH (6-2)	Mies
Taylor et al. (1999)	OH (6-2)	Mies and LWR
Shiokawa et al. (1999)	OH (6-2)	TL
Greet et al. (1998)	OH (6-2)	TL
Williams (1996)	OH (8-3)	Mies
Bittner et al. (2000)	OH (3-1)	Mies
Espy & Huppi (1997)	OH (3-1), OH (4-2)	Mies
Mulligan et al. (1995)	OH (3-1), OH (4-2)	TL and Nelson et al. (1990)

We designed and constructed a portable OH(8-3) rotational temperature photometer and installed it at Brazilian Antarctic station at King George Is. (62˚S, 50˚W) in 2000. Prior to that the photometer has been operated at Cachoeira Paulista airglow observatory (23˚S, 45˚W) for 4 months in 1999 in order to compare with the OH (6-2) rotational temperature observed at the same location. In the present work, therefore, we calculate the OH rotational temperature using the OH (8-3) and (6-2) band spectra, and compare between them using different Einstein coefficients published by Mies, TL and LWR.

INSTRUMENTATION AND DATA ACQUISITION

The portable photometer was designed to measure the OH (8-3) rotational temperature. It is a tilting filter photometer composed by an optics, photometer control electronics and data acquisition

systems. Figure 1 shows the schematic diagram of the photometer illustrating main part of the instrument. The optical system is composed by a near infrared interference filter with a diameter of 45 mm, 1.0 nm wavelength resolution, an objective lens, an internal calibration disk, a field stop diaphragm and a S20 PMT tube. The field of view is $2.5 \times 8°$, which corresponds to an area of about 4×12 km at the OH emission layer (around 87 km of altitude). The electronics controls PMT high voltage (HV), preamplifier (PA) and discriminator (Freq), as well as the step motor M1 for filter tilting and M2 for calibration disk rotating. All of the systems are controlled by a computer.

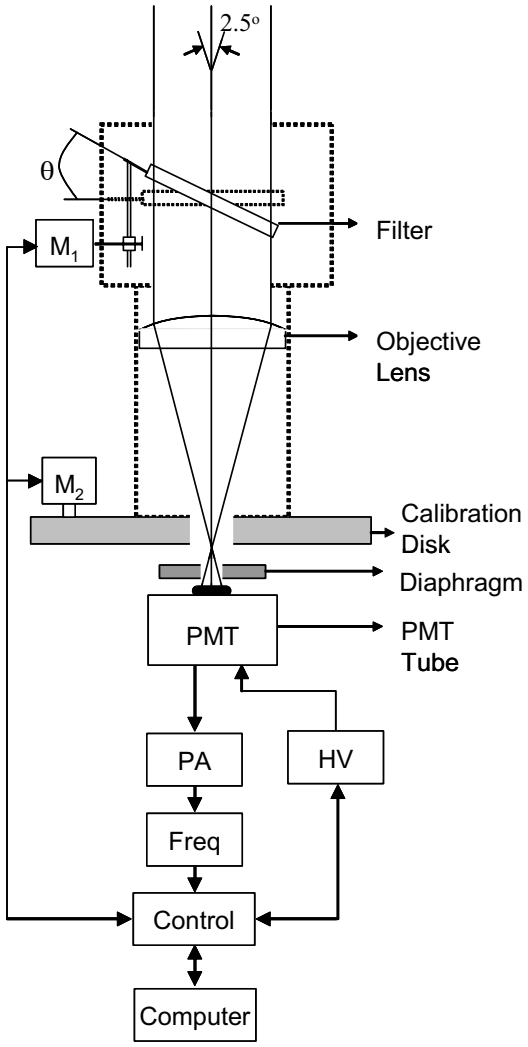

Figure 1 – Schematic diagram of the portable photometer illustrating the main parts of the equipment.

Figura 1 – *Esquema óptico e diagrama de blocos do fotômetro portátil.*

The photometer absolute sensitivity, counts/Rayleigh, was calibrated using a MgO screen illuminated by a laboratory substandard light source (Eppley ES 8315 calibration lamp). A tritium gas activated phosphor light source mounted in the disc was used for the day to day calibration of the sensitivity. The overall photometer sensitivity was around 3 counts/Rayleigh. This is low compared to the other ordinary airglow photometers, and requests longer time integration in order to get a good signal to noise ratio. One wavelength scan to get the $P_1(5)$ and $P_1(3)$ line spectra takes 20 seconds. After 10 continuous scanning an integrated spectrum is obtained, then the temperature was calculated. Estimated instrumental errors originating from filter transmission functions and uncertainty in the absolute sensitivity for the intensity and temperature are $\pm 6\%$ and ± 3 K, respectively, and the random error are $\pm 5\%$ and ± 6 K.

Fig. 2(A) shows an example of the OH(8,3) spectrum measured by the photometer, where the OH(8-3) P branch lines can be identified. The $P_1(3)$, $P_1(4)$ and $P_1(5)$lines can be traced by tilting the filter scanning the wavelength from 732 to 742 nm. The intensity ratio between $P_1(5)$ and $P_1(3)$ was used to calculate the rotational temperature, and this ratio has a larger temperature dependence compared to the other combination.

On the other hand, the OH (6-2) band $P_1(2)$, $P_1(3)$ and $P_1(4)$ lines were measured by MULTI-2, a tilting filter photometer, designed to scan the wavelength from 838 to 848 nm with the wavelength resolution of 1.0 nm (Melo et al., 1993). Fig. 2(B) shows a measured spectra of the OH(6-2) P branch. A large optical diameter (60 mm) and a high sensitivity PMT tube (GaAs) made it possible to achieve a reasonably high throughput, around 20 counts/Rayleigh, which is much higher than that of the portable photometer. A rectangular field of view of $2 \times 7°$ covers the OH emission layer with an area of 3×11 km over the zenith at $\sim$87 km of altitude. The intensity ratio between $P_1(4)$ and $P_1(2)$ was used to calculate the rotational temperature, which has a large temperature dependence compared to the other combinations such as $P_1(3)$ and $P_1(2)$. The $P_1(3)$ line was not used because of that there are $P_1(12)$ and $P_2(12)$ lines of the OH (5-1) band near of it at 843 nm, and it is difficult to estimate the contamination of these lines. Only a single scan was necessary to determine a temperature. Estimated instrumental errors originating from filter transmission functions and uncertainty in the absolute sensitivity for the intensity and temperature are $\pm 10\%$ and ± 2 K, respectively, and the random error ranges are $\pm 2\%$ and ± 3.5 K for each measurement (Takahashi, 1999).

The observations of the OH (6-2) band emission has been carried out at Cachoeira Paulista ($23°$S, $45°$W), during 1998 and 1999. A total of 107 nights of data, with more than 4 hours of continuous observation, was used in the present analysis. The simultaneous observations of the OH (8-3) and (6-2) band emis-

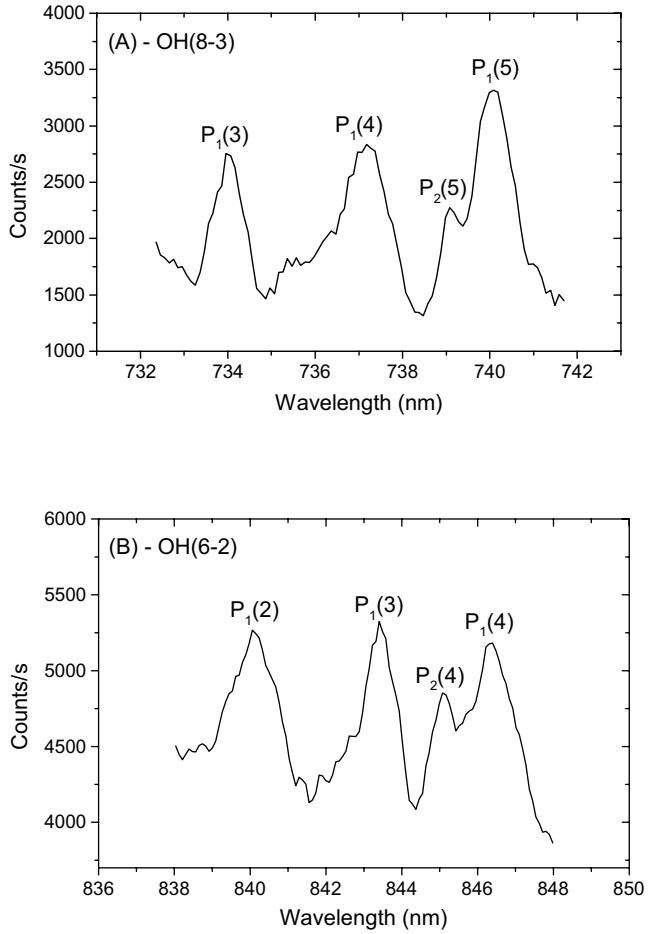

Figure 2 – (A) Typical spectra of the OH (8-3) observed by the portable photometer and (B) the spectra of the OH (6-2) observed by the MULTI-2 photometer, where are showing the main rotational lines in the P branch used to calculate the temperature of the (8-3) and (6-2) OH bands.

Figura 2 – *Em (A) é apresentado o espectro do OH (8-3) observado pelo fotômetro portátil e em (B) é apresentado o espectro do OH (6-2) observado pelo fotômetro MULTI-2, mostrando as principais linhas de emissão utilizadas para o cálculo da temperatura do OH(8-3) e OH(6-2).*

sions were carried out at the same place from August to November 1999. A total of 19 nights of data was obtained and used for the comparison. The three Einstein coefficients, Mies, TL and LWR, were used to compare the rotational temperature between them.

RESULTS AND DISCUSSION

The nocturnal mean values of the OH (8-3) rotational temperature (hereafter T_{83}) observed by the portable photometer from August to November 1999 are shown in Fig. 3(A). Temperatures calculated by using Mies, TL and LWR are plotted as a function of the observed intensity ratio between $P_1(5)$ and $P_1(3)$. The straight lines in the figure represent a linear trend of the temperatures. The figure shows that the temperatures calculated by the Mies coefficients are the lowest (circles) and the temperatures of the LWR coefficients are the highest (squares). The difference between them is not constant, but increasing with temperature, i.e., from 10 K around 180 K to 15 K around 230 K.

The nocturnal mean rotational temperatures of the OH (6-2) band (hereafter T_{62}) observed by MULTI-2 photometer between 1998 and 1999 are shown in Fig. 3(B). Different to the case of OH (8-3), the temperature using the Mies and LWR coefficients are lower than those obtained by TL. It should be pointed out that the temperature of LWR is almost the same to that of OH (8-3). The different temperature with different transition probabilities of the OH (6-2) band has already been reported by French et al. (2000).

In Table 2 overall averaged temperatures and the standard deviations of T_{83} and T_{62}, for the data from August to November 1999 are summarized. For T_{83} calculated using the LWR coefficient is 12 K higher than Mies and 3 K higher than TL. T_{62} using the TL coefficients is 13 K higher than LWR and 8 K higher than Mies.

Table 2 – Overall averaged rotational temperatures of the OH (8-3), T_{83}, and OH (6-2), T_{62}, and the standard deviation (SD), in Kelvin. Data: 19 nights from August to November 1999.

Tabela 2 – *Temperatura rotacional média de todas as noites da OH(8-3), T_{83}, e OH (6-2), T_{62}, e o desvio padrão (SD) em Kelvin. Dados coletados em 19 noites entre agosto e setembro de 1999.*

	T_{83}(K)		T_{62}(K)	
	Mean	SD	Mean	SD
Mies	196.8	11.5	214.1	8.3
TL	205.6	12.2	221.9	8.3
LWR	209.1	12.8	209.3	9.2

In order to compare the temperatures of the OH (8-3) and (6-2) emissions, the nocturnal mean values are plotted for the different transition probability groups, Mies, LWR, and TL, in Figure 4. As expected from the Figure 3, there is a good agreement in the mean temperatures between T_{83} and T_{62} for the LWR coefficients (209 K). For the Mies and TL coefficients, however, large differences in the temperatures, around 16 K, can be seen. The plots are rather scattered around the linear relation line in the figure. This might be due to the difference of random error range of the two different photometers. In Table 3, the difference in the temperature between T_{83} and T_{62} are summarized.

Table 3 – Temperature difference between OH (8-3) and OH (6-2) band.

Tabela 3 – *Diferença entre as temperaturas das bandas da OH (8-3) e OH (6-2).*

Einstein Coefficients	T_{62}-T_{83} (K)
LWR	+0.2
Mies	+17.2
TL	+16.2

The difference of temperature between the three transition probabilities, Mies, LWR and TL, shown in Fig. 3 are not observational result, but it came from the difference of the transition probabilities used as can be seen in the Eq.(1). It should be noted that the difference, more than 12 K, is large and we should keep in mind it when the OH rotational temperature is used to monitor the atmospheric temperature in a vicinity of the mesopause around 85 to 90 km.

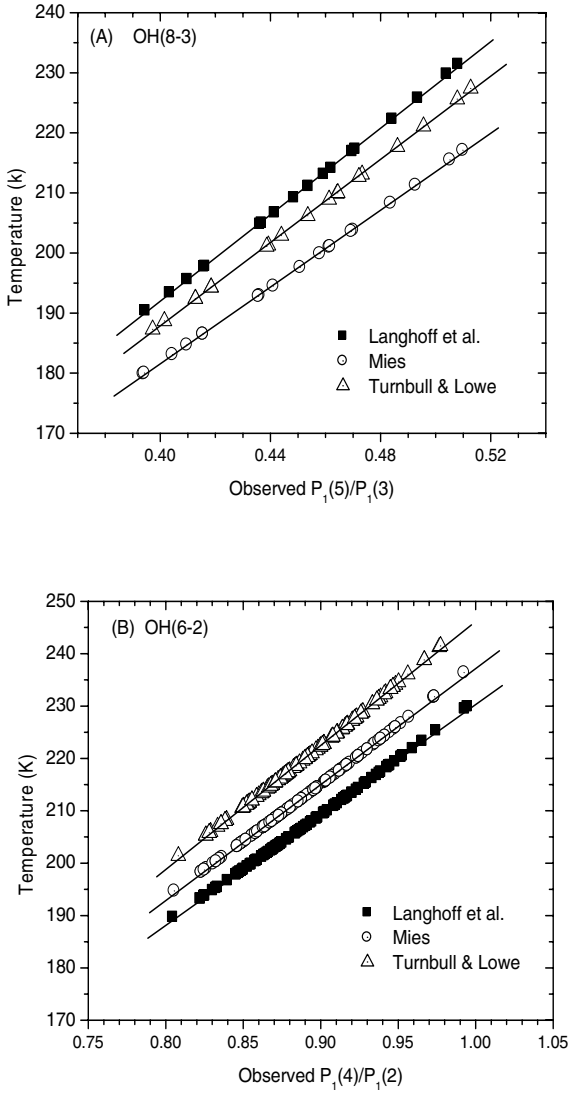

Figure 3 – Nocturnal mean rotational temperatures as a function of the observed intensity ratio for the different Einstein coefficients, Mies (1974), Langhoff et al. (1986) and Turnbull & Lowe (1989), of the OH (8-3) band (A), and (B) of the OH (6-2) band, observed at Cachoeira Paulista (23˚S, 45˚W).

Figura 3 – *(A) Média noturna da temperatura rotacional da OH (8-3) em função das razões de intensidades observadas para os diferentes coeficientes de Einstein de Mies(1974), Langhoff et al. (1986) e Turnbull & Lowe (1989). Em (B) o mesmo para a banda da OH (6-2). Os dados foram obtidos em Cachoeira Paulista (23˚S, 45˚O).*

The difference of temperature between the OH (8-3) and (6-2) emissions from one transition probability to the others showed in the Fig. 4 is significant. A good agreement between the two temperatures can be seen in the case of LWR. The small difference of 0.2 K should not be called much attention if we look into the scattered points in the Fig. 4 and the instrumental error ranges of the two photometers, which is around $\pm$5 K. The temperature differences larger than 16 K in the case of the Mies and TL tran-

sition probabilities, however, are much larger than expected from the instrumental error range.

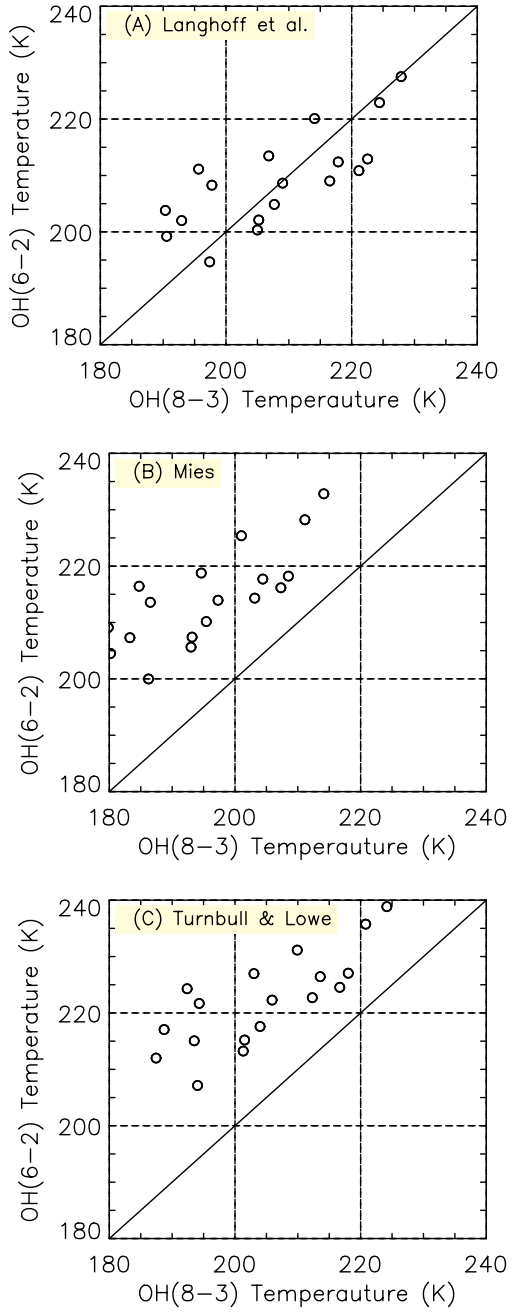

Figure 4 – Comparison of the observed OH (8-3) and (6-2) temperatures using Langhoff et al. (1986) transition probabilities (A), Mies (1974) (B), and Turnbull & Lowe (1989) (C).

Figura 4 – *Comparação da temperatura rotacional das bandas da OH (8-3) e (6-2) usando os coeficientes de Einstein de Langhoff et al em (A), Mies (1974) em (B) e Turnbull & Lowe (1989) em (C).*

There is another possibility to give a different temperature in the two emissions. If the emission heights are different and the atmospheric temperature has a gradient with height, the weighted mean temperatures of the two bands could be different. Past rocket measurements (Lopez-Moreno et al., 1987) report that the difference between the emissions from the upper vibrational levels ($\nu = 7$) and the lower ones ($\nu = 2$) could be as much as 5 km. On the other hand, McDade (1991), concluded that the height difference from the upper vibrational level ($\nu = 9$) to the lower one ($\nu = 1$) should not be more than one or two kilometers. Whether the two emission layers are different with height or not, we can check it by looking into phase difference of their nocturnal intensity variations. In case of the gravity waves and tidal oscillations, their phase propagations are normally from the upper to lower heights. If the OH (8-3) emission profile is higher than OH (6-2), the former leads the latter. In order to check it, the intensity variations of the 19 nights were investigated using time lagged cross correlation analysis. No significant time lag (larger than 10 minutes) between the two emissions was found. In Fig. 5 typical nocturnal variations of the intensity and the rotational temperature on the night of September 3 and 4 are shown. Well correlated variation patterns of the OH (8-3) and (6-2) intensities can be seen. For the temperature calculation the LWR coefficients were used for both the emissions. The large variance of T_{83} is due to the low signal to noise ratio of the OH (8-3) band observation on this night, resulting in a larger random error. From these results we conclude that the difference in the temperature between OH (8-3) and (6-2) should not be caused by their height difference and possible temperature gradient, neither the instrumental errors. The difference should be originated from the transition probabilities used. French et al. (2000) reported that the OH (6-2) band temperature calculated by LWR had a better agreement with their experimental values than those calculated by Mies and TL. Our present results and their discussion, therefore, lead a conclusion of that the LWR transition probabilities should provide a temperature of the OH emission layer better than the others, at least for the case of OH (8-3) and (6-2) band observations. For comparison of the present OH rotational temperatures with model atmosphere, the temperatures of MSIS-90 (Hedin, 1991) are also plotted in the figure. The MSIS-90 temperature shows similar nocturnal variation, but with much lower values, $\sim$ 20 K, compared to the OH rotational temperature, which should be further investigated.

CONCLUSION

The OH rotational temperatures were calculated from simultaneously observed OH (8-3) and (6-2) band P branch spectra. Rotational temperature of the OH (8-3) band calculated by three diffe-

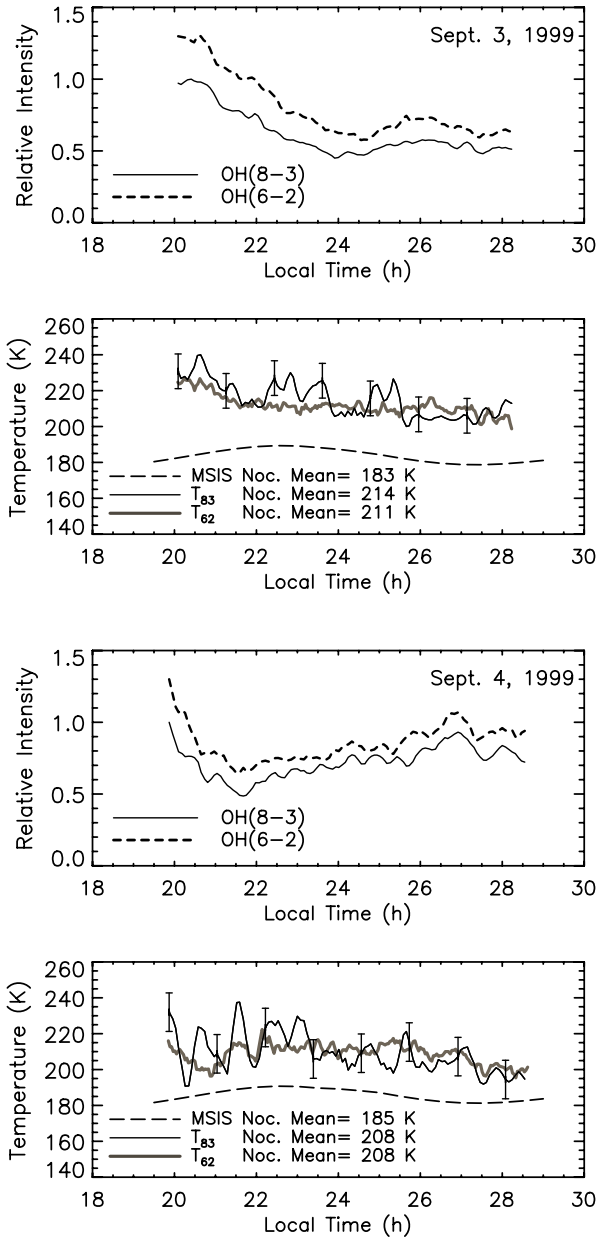

Figure 5 – Nocturnal variations of the OH (8-3) and (6-2) band intensities and rotational temperatures observed at Cachoeira Paulista on September 3rd and 4th, 1999. Transition probabilities used are given by Langhoff et al. (1986). The rotational temperatures are also compared with the MSIS-90 model that showed the lowest values of temperature. The local time is expressed in decimal time and varies from 18 to 30 hours (18 to 06 hours of the next day).

Figure 5 – *Variações noturnas da intensidade e da temperatura rotacional das bandas da OH (8-3) e da OH (6-2) observadas em Cachoeira Paulista nas noites de 03 e 04 de setembro de 1999, utilizando os Coeficientes de Einstein dados por Langhoff et al. (1986). As temperaturas rotacionais são comparadas com o modelo MSIS-90, que apresenta os menores valores de temperatura. A hora local é expressa em hora decimal que varia das 18 às 30 horas (18 às 06 horas do dia seguinte).*

rent Einstein coefficients show that the LWR coefficients provide the highest values and the Mies provides the lowest values. For the OH (6-2) band the higher temperatures values are from the TL coefficients and the lowers due the LWR coefficients. A good agreement in the rotational temperatures between the OH (8-3) and (6-2) bands was obtained when the LWR coefficients were used. The portable OH temperature photometer is in operation at Brazilian Antarctic Station (62˚S, 58˚W) since 200. The temperature data are available under request to authors.

ACKNOWLEDGEMENTS

The present work has been supported by CAPES and CNPq, under contract PROANTAR project No. 55.0355/02-2.

REFERENCES

BAKER DJ & STAIR JAT. 1988. Rocket Measurements of the Altitude Distributions of the Hydroxyl Airglow. Physica Scripta, 37(4): 611–622.

BITTNER M, OFFERMANN D & GRAEF H. 2000. Mesopause temperature variability above a midlatitude station in Europe. Journal of Geophysical Research, 105(D2): 2045–2058.

ESPY PP & HUPPI R. 1997. The intertropical convergence zone as a source of short-period mesospheric gravity waves near the equator. Journal of Atmospheric and Solar-Terrestrial Physics, 59(13): 1665–1671.

FRENCH WJR, BURNS GB, FINLAYSON K, GREET PA, LOWE RP & WILLIAMS PFB. 2000. Hydroxyl (6-2) airglow emission intensity ratios for rotational temperature determination, Annales Geophysicae, 18(10): 1293–1303.

GOLDEN SA. 1997. Kinetic parameters for OH nightglow consistent with recent laboratory measurements. Journal of Geophysical Research, 102(A9): 19969–19976.

GREET PA, FRENCH WJR, BURNS GB, WILLIAMS PFB, LOWE RP & FINLAYSON K. 1998. OH (6-2) spectra and rotational temperature measurements at Davis, Antarctica. Annales Geophysicae, 16(1): 77–89.

HEDIN AE. 1991. Extension of the MSIS Thermosphere Model into the Middle and Lower Atmosphere, Journal of Geophysical Research, 96(A2): 1159–1172.

LANGHOFF SR, WERNER HJ & ROSMUS P. 1986. Theorical transitions-probabilities for the OH Meinel system. Journal of Molecular Spectroscopy, 188(2): 507–529.

LOPEZ-MORENO JJ, RODRIGO R, MORENO F, LOPEZ-PUERTAS M & MOLINA A. 1987. Altitude distribution of vibrationally excited states of atmospheric hydroxyl at levels v = 2 to v = 7, Planet. Space Sci., 35: 1029–1038.

MCDADE IC. 1991. The altitude dependence of the OH (X2PI) vibrational distribution in the Nightglow: Some model expectations., Planet. Space Sci., 39: 1049–1057.

MEINEL AB. 1950. OH Emission Bands in the Spectrum of the Night Sky. I, Transactions-American Geophysical Union, 31 (21).

MIES FH. 1974. Calculated vibrational transitions probabilities of OH ($X^2\Pi$). Journal of Molecular Spectroscopy, 53: 150–188.

MELO SML, GOBBI D, TAKAHASHI H, TEIXEIRA NR, LOBO R. 1993. O fotômetro MULTI-2 Experiência de calibração – 1992. São José dos Campos: INPE, (INPE-5526, NCT/310).

MULLIGAN FJ, HORGAN DF, GALLIGAN JG & GRIFFIN EM. 1995. Mesopause temperatures and integrated band brightness calculated from airglow OH emission recorded at Maynooth (53,2˚N, 6.4˚W) during 1993. Journal of Atmospheric and Solar-Terrestrial Physics, 57(13): 1623–1637.

NELSON DD, SCHIFFMAN A, NESBIT DJ, ORLANDO JJ & BURKHOLDER JB. 1990. H + O_3Fourier-transform infrared emission and laser absorption studies of OH ($X^2\Pi$) radical: An experimental dipole moment function and state-to-state Einstein A coefficients. Journal of Chemical Physics, 93(10): 7003–7019.

SCHEER J & REISIN SR. 2000. Unsual low airglow intensities in the Southern Hemisphere midlatitude mesopaude region. Earth Planets and Space, 52(4): 261–266.

SHIOKAWA K, KATOH Y, SATOH M, EJIRI MK, OGAWA T, NAKAMURA T, TSUDA T & WIENS RH. 1999. Development of Optical Mesosphere Thermosphere Imagers (OMTI). Earth Planets and Space, 51(7-8): 887–896.

SIVJEE GG & HAMWEY RM. 1987. Temperature and chemistry of the polar mesopause OH. Journal of Geophysical Research, 92(A5): 4663–4672.

TAKAHASHI H, BATISTA PP, BURITI RA, GOBBI D, NAKAMURA T, TSUDA T & FUKAO S. 1998. Simultaneous measurements of airglow OH emission and meteor wind by a scanning photometer and the MU radar. Journal of Atmospheric and Solar-Terrestrial Physics, 60(17): 1649–1668.

TAKAHASHI H, BATISTA PP, BURITI RA, GOBBI D, NAKAMURA T, TSUDA T & FUKAO S. 1999. Response of the airglow OH emission, temperature and mesopause wind to the atmospheric wave propagation over Shingaraki, Japan. Earth Planets and Space, 51(7-8): 863–875.

TAYLOR MJ, PENDLETON WR-JR., GARDNER CS & STATES RJ. 1999. Comparison of diurnal tidal oscillations in mesospheric OH rotational temperature and Na lidar temperature measurements at mid-latitudes for fall/spring conditions. Earth Planets and Space, 51(7-8): 877–885.

TURNBULL DN & LOWE RP. 1989. New hydroxyl transitions probabilities and this importance in airglow studies. Planetary and Space Science, 37(6): 723–738.

WALTERSCHEID RL, SCHUBERT G & STRAUS JM. 1987. A dynamical-chemical model of the wave-driven fluctuations in the OH nightglow. Journal of Geophysical Research, 92(A2): 1241–1254.

WILLIAMS PFB. 1996. OH rotational temperatures at Davis, Antarctica, via scanning spectrometer. Planetary and Space Science, 44(2): 163–170.

NOTES ABOUT THE AUTHORS

Cristiano Max Wrasse. Physicist at Universidade Federal de Santa Maria (UFSM), 1997. Msc (Space Geophysics) at Instituto Nacional de Pesquisas Espaciais (INPE), 2000. PhD (Space Geophysics) at Instituto Nacional de Pesquisas Espaciais (INPE), 2004. Areas of interest: Equatorial and Polar Optical Aeronomy.

Hisao Takahashi. Bsc (Physics) at Niigata University – Japan, 1968. Msc (Upper Atmosphere) at Niigata University – Japan, 1970. PhD. (Space Science) at Instituto de Pesquisas Espaciais – INPE, 1980. Areas of interest: Optical Aeronomy.

Delano Gobbi. Bsc (Physics) at Universidade Federal do Rio Grande do Sul, UFGRS, 1984. Msc (Space Science) at Instituto de Pesquisas Espaciais, (INPE), 1988. PhD (Space Science) at Instituto de Pesquisas Espaciais, (INPE), 1993. Areas of interest: Equatorial and Polar Optical Aeronomy.